Chinese Chemical Letters 34 (2023) 108072

Contents lists available at ScienceDirect

Chinese Chemical Letters

journal homepage: www.elsevier.com/locate/cclet

Strategic design of lysine-targeted irreversible covalent NDM-1 inhibitors

Youzhen Ma[a], Yongxi Liang[a], Menglu Guo[a], Delin Min[a], Lulu Zheng[c], Yun Tang[c], Xun Sun[a,b,*]

[a] Department of Natural Medicine, School of Pharmacy, Fudan University, Shanghai 201203, China
[b] The Institutes of Integrative Medicine of Fudan University, Shanghai 200040, China
[c] Shanghai Key Laboratory of New Drug Design, School of Pharmacy, East China University of Science and Technology, Shanghai 200237, China

ARTICLE INFO

Article history:
Received 30 August 2022
Revised 24 November 2022
Accepted 12 December 2022
Available online 14 December 2022

Keywords:
Covalent inhibitors
Lysine
Irreversible
Metallo-β-lactamase
Antimicrobial activity

ABSTRACT

New Delhi metallo-β-lactamase 1 (NDM-1) can hydrolyze most β-lactam antibiotics, which is the major factor for drug resistance of Gram-negative bacteria. The binding of most reversible inhibitors to NDM-1 is relatively weak due to the shallow active pocket of NDM-1. Alternatively, irreversible covalent inhibitors can prevent their dissociation from the target, leading to permanent inactivation of the protein. Herein, we report a series of irreversible covalent inhibitors of NDM-1 targeting the conserved Lys211 in the active pocket. Several methods, including mass spectrometry, sodium dodecyl sulfate-polyacrylamide gel electrophoresis, fluorescent labeling, and coumarin probe were used to demonstrate that pentafluorophenyl ester formed a covalent bond with Lys211. Moreover, our target inhibitor, in combination with meropenem, achieved an antibacterial effect on drug-resistant bacteria, along with an excellent safety profile. Our new strategy in designing lysine-targeted irreversible covalent NDM-1 inhibitors provides a potential option for the clinical treatment of Gram-negative bacteria.

New Delhi metallo-β-lactamase 1 (NDM-1) exists in Gram-negative bacteria, such as *Escherichia coli* (*E. coli*) or *Klebsiella pneumoniae* (*K. pneumonia*). As a Zn(II)-containing enzyme, NDM-1 can inactivate β-lactam antibiotics through opening the β-lactam ring by a nucleophilic water, making these so-called super bacteria resistant to most β-lactam antibiotics including carbapenems. As a result, limited clinical drugs can be applied to fight such infections [1,2]. Two general types of inhibitors against hydrolases, either reversible or irreversible, are usually designed to target catalytic nucleophilic amino acids, such as serine and cysteine residues. For example, the approved serine-β-lactamases (SBLs) inhibitors such as Avibactam, Vaborbactam [3,4], were based on covalent bond formation from the nucleophilic serine at the catalytic site.

Unlike the formation of a covalent bond from serine in SBLs, the active site of metallo-β-lactamases (MBLs) utilizes a water molecule chelated by two Zn(II) ions to hydrolyze the β-lactam ring. In other words, conventional design strategies for covalent inhibitors of amidohydrolases are not applicable to NDM-1. At present, most MBLs inhibitors are non-covalent inhibitors, such as L-Captopril, Thiorphan and Taniborbactam [5,6]. Since the active pocket of NDM-1 is a shallow groove, the binding of reversible inhibitors to NDM-1 is relatively weak [7]. Therefore, it is challenging and important to develop irreversible covalent inhibitors against MBLs.

The crystal structures of MBLs indicate the active pocket contains a series of nucleophilic amino acids, such as cysteine and lysine, which can be targeted by covalent inhibitors. Because the conserved lysine at the bottom of the active pocket plays a critical role in substrate binding [8], the covalent targeting of these amino acids can be an efficient strategy to inhibit the catalytic activity of MBLs. As shown in Fig. 1, some covalent MBLs inhibitors have been reported in this field, with compounds **1-4** targeting lysine residues and compounds **5-8** targeting cysteine residues in the active pocket [9–14]. Most of these inhibitors are early hits from high-throughput screening, so they often suffer from low activity against NDM-1, poor water solubility, or selectivity issues. For example, the thiol groups of **3** and **4** tend to bind to other enzymes containing Zn(II), resulting in toxic side effects [15].

Herein we report an irreversible covalent inhibitor of NDM-1 with cephalosporin as the core backbone and an active ester as a covalent warhead. Compared with the reported non-covalent inhibitors, such as metal chelators and sulfhydryl compounds, and covalent inhibitors, such as *p*-chloromercuric benzoic acid and ebselen [13,16], cephalosporins have little effect on the other en-

* Corresponding author.
E-mail address: sunxunf@shmu.edu.c (X. Sun).

https://doi.org/10.1016/j.cclet.2022.108072
1001-8417/

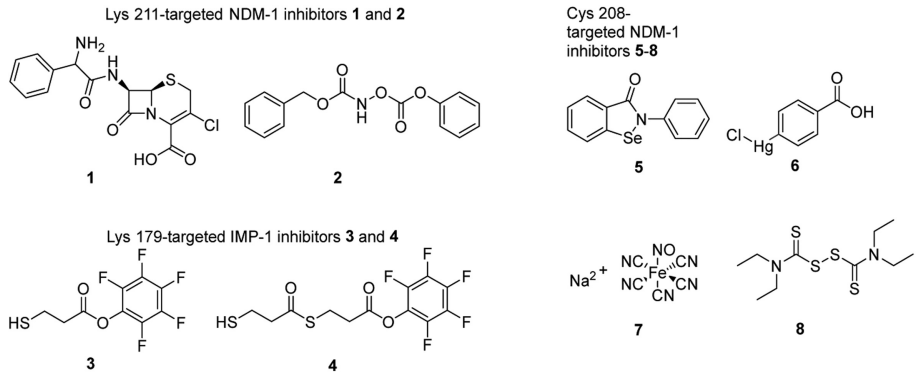

Fig. 1. The structure of covalent inhibitors of MBLs.

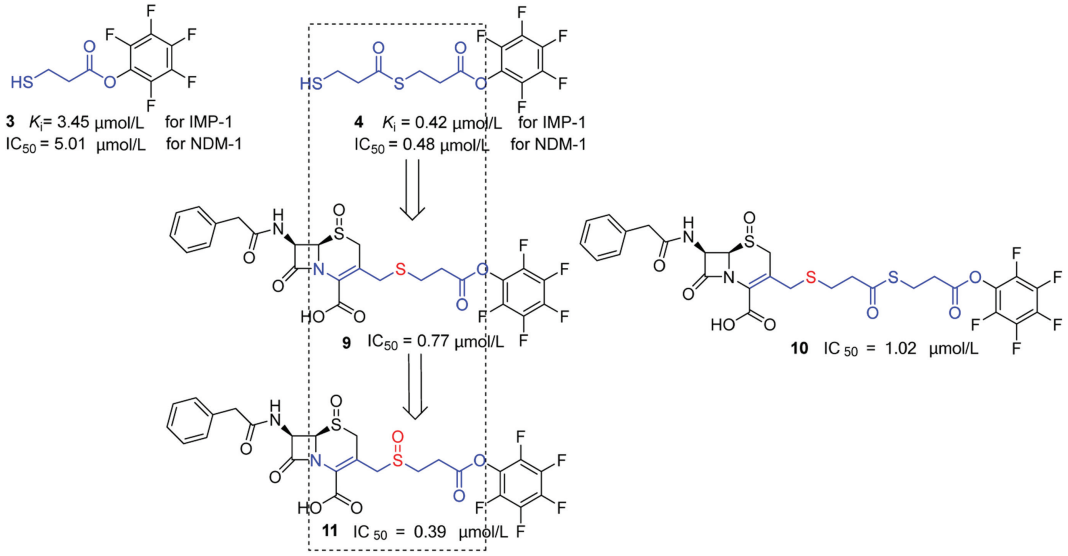

Fig. 2. The design and structure-activity relationships of NDM-1 inhibitors.

zymes containing Zn(II) or cysteine. Thus, our strategy for new covalent NDM-1 inhibitors is to combine cephalosporin and a pentafluorophenyl active ester, a key unit in compounds **3** and **4** as a covalent warhead targeting IMP-1 lysine.

The K_i values for IMP-1 inhibitors **3** and **4** were reported to be 3.5 μmol/L and 0.4 μmol/L, respectively [11]. Given the structural similarity between NDM-1 and IMP-1 (Fig. S1 in Supporting information), we tested **3** and **4** for the inhibition of NDM-1, with IC_{50} of 5.0 μmol/L and 0.5 μmol/L, respectively (Figs. S2A and B in Supporting information). Unfortunately, neither **3** nor **4** potentiated the efficacy of meropenem (MER) against clinical isolates harboring NDM-1 (Table S1, Figs. S3A-C in Supporting information). Therefore, the sulfhydryl group was replaced with a cephalosporin backbone, aiming for potential binding to the active pocket of NDM-1, meanwhile, the pentafluorophenyl active ester was maintained for the potential formation of an irreversible covalent bond with Lys211. As a result, compounds **9** and **10** (Fig. 2) were designed and synthesized, in which the sulfur atom in the bicyclic skeleton was oxidized to (*S*)-sulfoxide to avoid Δ_2-Δ_3 isomerization and reduce the spontaneous hydrolysis rate [17,18].

Next, the inhibitory activities of **9** and **10** against NDM-1 were tested, with IC_{50} of 0.8 μmol/L and 1.0 μmol/L, respectively (Figs. S2C and D in Supporting information). Surprisingly, upon the replacement of thiol group in **3** with cephalosporin backbone, the inhibitory activity of **9** against NDM-1 significantly increased by 6.5-fold, while **10** showed slightly lower activity than **4** after similar substitution. The comparable IC_{50} values between **4** and **9** could be explained by their similar binding modes. The thiol group in **4** and the cephalosporin backbone in **9** are coordinated with the Zn(II). Through the same distance from the Zn(II), the active ester in both compounds can form a stable covalent bond with the Lys211 of NDM-1. It was known that **9** would liberate pentafluorophenyl mercaptopropionate (**3**) upon the hydrolysis of β-lactam ring by NDM-1 (Scheme S1 in Supporting information) [19], and the resultant pentafluorophenyl mercaptopropionate did not potentiate the minimum inhibitory concentration (MIC) of meropenem against clinical isolates harboring NDM-1. In order to prevent the cleavage of such a thioether after hydrolysis of the β-lactam ring in **9**, we oxidized the sulfur atom to sulfoxide to obtain compound **11** (Fig. 2), which was a pair of diastereomers (67.1:32.9) due to the stereocenter at sulfur (Fig. S7 in Supporting information). As a result, this NDM-1 inhibitor **11** can not only bind to the Zn(II) in the active pocket, but also form a covalent bond with the conserved Lys211 no matter whether the β-lactam ring is hydrolyzed or not. The IC_{50} of **11** against NDM-1 was determined to be 0.4 μmol/L (Fig. S2E in Supporting information).

Subsequently, we explored the binding mode of **11** with NDM-1 by covalent docking using Schrodinger software. The docking model (Fig. 3) showed the existence of two hydrogen bonds: the carbonyl oxygen atom of phenylacetamide region with Gln123, and the carboxyl oxygen atom of cephalosporin region with Asn220. At the same time, two Zn(II) ions formed coordination bonds with the oxygen atoms of the β-lactam ring and the carboxyl group, respectively. More importantly, in addition to the above conventional in-

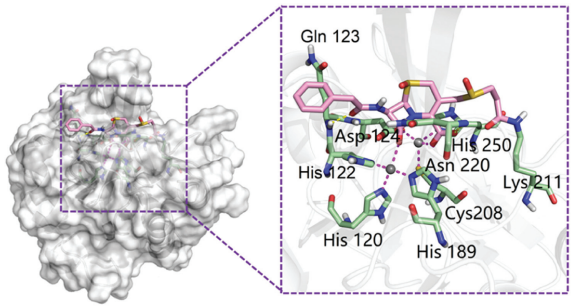

Fig. 3. Binding model of NDM-1 and irreversible inhibitor **11** generated using Schrodinger Maestro and Pymol, only key residues are shown, hydrogens of ligand omitted for clarity.

teractions, the active ester was displaced by Lys211 to form a covalent bond as expected. By overlapping the docking model with the crystal structure of 6OVZ (Fig. S4 in Supporting information), we found that the fundamental morphology of Lys211 almost remained unchanged after the covalent bond formation between **11** and Lys211, indicating that the covalent binding did not cause unreasonable alteration in protein conformation.

Next, we focused on confirming the covalent interaction of **11** with NDM-1, we evaluated the incubation of **11** with NDM-1 using polyacrylamide gel under denaturing conditions. The change in molecular weight of NDM-1, after the formation of a covalent adduct with **11**, would lead to different moving behaviour on polyacrylamide gels [20]. In this case, pure NDM-1 and incubation of NDM-1 with **11** in 20 mmol/L Tris-HCl (pH 7.5) at 25 °C were evaluated by polyacrylamide gel. The results (Fig. S5 in Supporting information) showed that the adduct of NDM-1 with **11** moved slightly slower, with multiple repetitions, than NDM-1, indicating that **11** formed covalent adduct with NDM-1.

To further confirm the formation of the covalent bond between **11** and the lysine of NDM-1. The trypsin digestion of NDM-1, with or without treatment by **11**, was analyzed by LC/MS/MS. Obviously, peptide sequence analysis showed that the trypsin-digested NDM-1 contained the peptide of Lys211. Due to potential fragmentation during the ionization process in LC/MS/MS, no peptides labelled with **11** were detected in the trypsin-digested incubation of NDM-1 upon treatment with **11**. However, the covalent bond formation with **11** was supported according to the subsequent analysis by primary mass spectrometry. The ionization showed the parent peak for NDM-1 (27634.4252) and an adduct peak (28015.1483), with the difference as 380.7231 (Fig. 4A). A possible explanation was illustrated in Fig. 4B [21]. The mass of initial adduct **11-1** derived from the active ester **11** was 450.0555 higher than NDM-1. Upon the hydrolysis of β-lactam ring and subsequent decarboxylation, the adduct of **11-4** was formed, with molecular weight 380.0864 higher than NDM-1. This data was consistent with what we observed in the primary mass spectrometry, and indicated that NDM-1 only bound one equivalent of **11**.

In addition, a fluorescent labelling analogue **12** was synthesized by replacing the benzene ring in **11** with a dansylamide moiety (Fig. 5A). This compound could also form a covalent bond with lysine in NDM-1, thus displaying fluorescence under excitation by UV light [22,23]. Upon the pre-treatment of NDM-1 with vehicle or **11** for 40 min, respectively, the subsequent incubation with **12** was conducted in 20 mmol/L Tris-HCl (pH 7.5) at 25 °C for 1 h. As shown in polyacrylamide gels under denaturing conditions (Fig. 5B), no fluorescence was observed at all for the NDM-1 lane. On the other hand, the incubation of NDM-1 with **12** presented obvious fluorescence, and the corresponding NDM-1 band was detected after Coomassie staining (Fig. 5B). When NDM-1 was pretreated with **11** prior to labelling with **12**, the fluorescent band of NDM-1 gradually became weaker as the concentrations of **11** increased (Fig. 5B), suggesting the formation of covalent bond with lysine already took place with **11** in the active pocket of NDM-1 and less free lysine residues were available for **12** to react with. These results indicated that **12** formed a covalent bond with the lysine in the active pocket of NDM-1.

Another fluorescent probe **13**, in which 7-hydroxycoumarin was introduced for potential cyan fluorescence, was prepared (Fig. 5A). Instead of pentafluorophenol, the formation of a covalent bond between **13** and the lysine in NDM-1 will release 7-hydroxycoumarin (Scheme S2 in Supporting information), which can be monitored by spectrofluorophotometer [24]. As a result, the fluorescence value (at 460 nm) of the incubation **13** with NDM-1 significantly increased in a time-dependent manner and reached 9997 a.u. at 70 min, indicating that **13** formed an amide bond with NDM-1 (Fig. 5C). On the other hand, the fluorescence value of **13** without NDM-1 changed little with time and stayed below 2000 a.u. at 70 min (Fig. 5C). These results further demonstrated that **11**, with a similar structure to probe **13**, was able to form a covalent bond with NDM-1.

Furthermore, we would figure out the exact lysine site in NDM-1 for **11** and **12** to form a covalent bond. According to literature reports, NDM-1 has three potential sites (Lys211, Lys214 and Lys216) [25], and LC/MS experiment demonstrated that NDM-1 only binds to one equivalent of **11**, but the exact lysine it acts on has not been identified. It is well known that three proteins in B1 subclass, NDM-1, VIM-2 and IMP-1, have similar activity pockets. The sequence homologies of NDM-1 with IMP-1 and VIM-2 are 30% and 33%, respectively (Table S2 in Supporting information) [7]. Further analysis revealed that IMP-1 and VIM-2 do not contain lysine residues corresponding to Lys214 and Lys216 residues of NDM-1, and Lys211 of NDM-1 corresponds to Lys179 of IMP-1 and Tyr201 of VIM-2, respectively (Table S3 in Supporting information) [7]. In order to understand the covalent bond formation, these three proteins were subjected to labelling experiments with **12**, and the results showed that **12** has approximately the same labelling effect on NDM-1 and IMP-1, suggesting the same covalent chemistry of Lys211 in NDM-1 and Lys179 in IMP-1. Meanwhile, the labelling effect on VIM-2 was much weaker (Fig. 5D), owing to the less reactive Tyr201 in VIM-2. These experimental results confirmed the decisive role of Lys211 in the fluorescent labelling of NDM-1, and further demonstrated that Lys211 was the site for covalent bond formation of **12** with NDM-1.

Next, we turned to evaluate the synergistic inhibitory effect of **9** and **11**, in combination with MER, against *E. coli* and *K. pneumoniae* harboring NDM-1. The combination of **11** (at 32 μg/mL) with MER could reduce the MIC of MER against *E. coli* BL21 (NDM–1^+) and clinical isolates *E. coli* BAA-2452 (bla_{NDM-1}) by 128-fold and 8-fold, respectively (Figs. 6A and B). Meanwhile, **9** showed a relatively weak synergistic antibacterial effect against *E. coli* BL21 (NDM–1^+) (Fig. S3D and Table S1 in Supporting information). As shown in the Figs. 6A and B, **11** almost exhibited no bacteriostatic effect even at 128 μg/mL in the absence of MER, suggesting that the **11** with lower toxicity restored the antibacterial activity of MER by inhibiting NDM-1.

Due to limited reports on the safety of covalent inhibitors targeting lysine, we profiled the cytotoxicity of **11** against tumor cells SGC-7901 and HT-29 at 4 μmol/L, 40 μmol/L, and 200 μmol/L concentrations. Viability of SGC-7901 and HT-29 was greater than 60% in the presence of 200 μmol/L **11**, and limited inhibitory effect was observed on the proliferation of SGC-7901 and HT-29 (Figs. S6A and B in Supporting information). In addition, **11** had no cardiotoxicity concern, with hERG IC_{50} much greater than 40 μmol/L (Fig. S6C in Supporting information). A single-dose acute toxicity experiment was conducted with C57BL/6 mice, and **11** did not induce a significant effect on the weight, activity and mental state

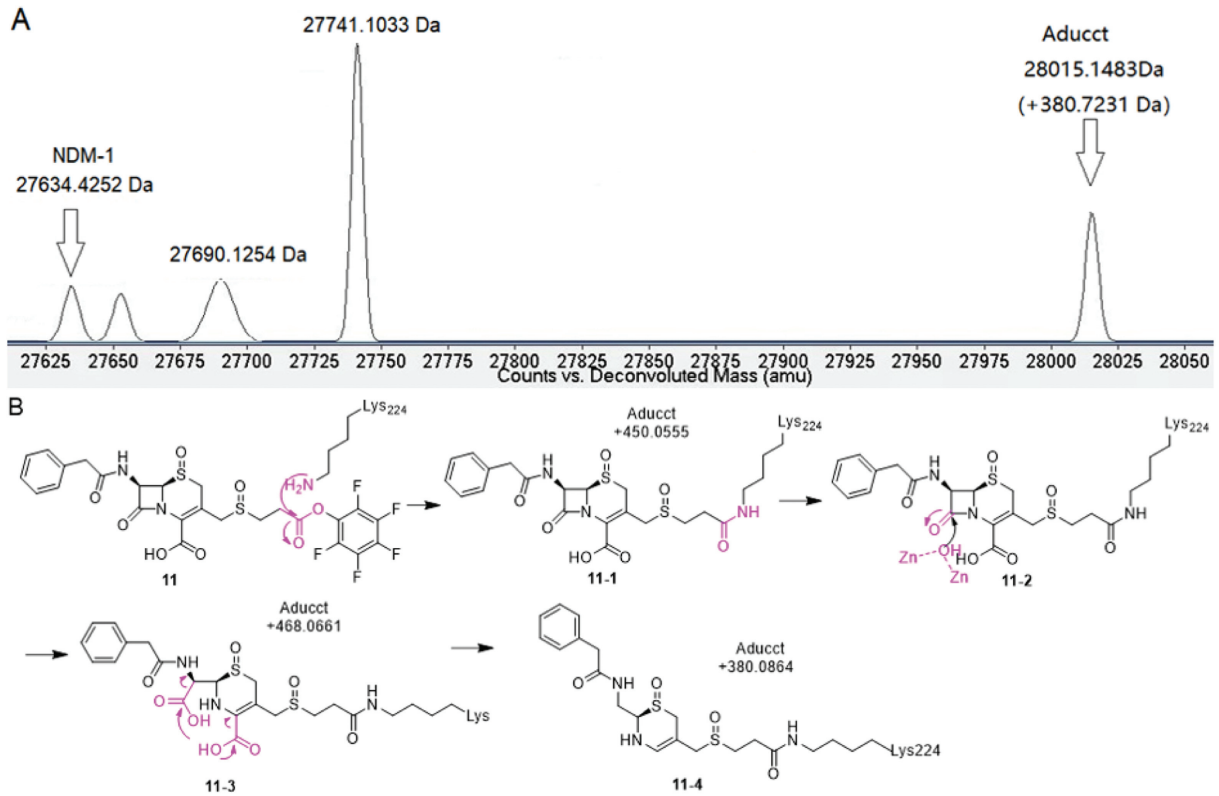

Fig. 4. (A) Extracted mass ionization chromatogram from incubation mixture of NDM-1 with **11**; (B) Degradation process after the interaction of compound **11** with NDM-1.

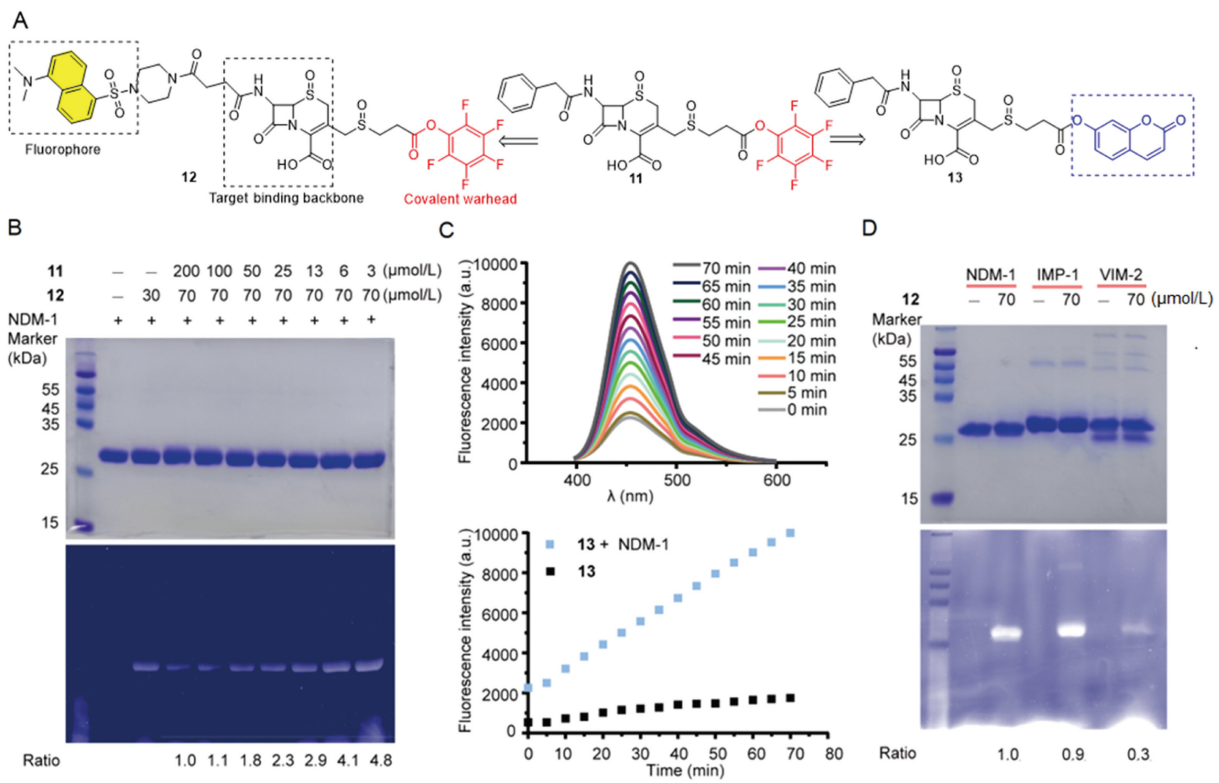

Fig. 5. Covalent binding of **12** and **13** to MBLs established by SDS-PAGE and fluorescence. (A) The structures of **12** and **13**; (B) Fluorescence imaging and Coomassie staining; Ratio is defined as the grayscale analysis of fluorescence (bottom) divided by the grayscale analysis of Coomassie blue staining (top); (C) Time-dependent emission spectra of **13** in the presence and absence of NDM-1; (D) Fluorescence imaging and Coomassie staining of NDM-1, IMP-1 and VIM-2 treated with **12**.

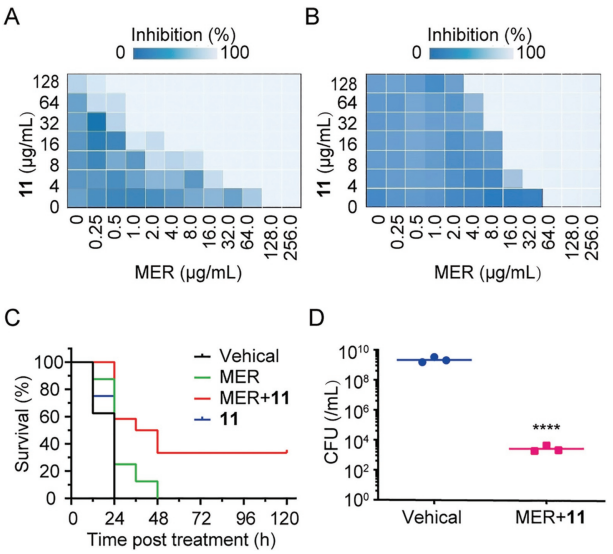

Fig. 6. **11** boosted the antimicrobial activity of MER *in vitro* and *in vivo*. (A, B) Representative heat plots of microdilution checkerboard assay for the combination of MER and **11** against *E. coli* BL21 (NDM-1$^+$), *E. coli* BAA-2452. (C) Survival curves showing efficacies in a murine peritonitis infection model with the use of cyclophosphamide. BALB/c mice were infected by a lethal dose of *E. coli* BAA-2452 *via* intraperitoneal injection. Four groups of mice were treated with vehicle control, monotherapy of MER (10 mg/kg), **11** (20 mg/kg), or combination therapy of MER and **11**. Eight mice per group were used in vehicle control, monotherapy of MER, or 12 mice per group in the combination therapy. (D) 4 h after mice were injected intraperitoneally with *E. coli* BAA-2452, blood was taken to detect the number of bacteria. 5 days after administration, blood was taken from the surviving mice to detect the number of bacteria. $^{****}P < 0.0001$, *t*-test, significant difference from the vehicle group.

of the mice (Table S4 in Supporting information), except that some body weight loss was observed for the mice at 400 mg/kg dose group at 8-11 days of administration (Fig. S6D in Supporting information). Overall, **11** displayed a good safety profile.

In addition, we investigated the potential *in vivo* benefit of this combination therapy in BALB/c mice using an intraperitoneal infection model. The results showed that the combination of **11** with MER, through intraperitoneal injection, could improve the survival rate of *E. coli* BAA-2452 intraperitoneal infected mice (Fig. 6C). Meanwhile, the number of bacteria in the blood of survival mice was significantly reduced after five days of administration. (Fig. 6D).

In conclusion, an irreversible covalent inhibitor **11**, utilizing cephalosporin as the backbone and active ester as a covalent warhead, was rationally designed to specifically target the Lys211 residue in the active pocket of NDM-1. This tool compound enabled breakthrough studies, from enzymatic to bacterial inhibition *in vitro* and *in vivo*, for lysine-targeted covalent inhibitors of NDM-1. Notably, the cephalosporin-based strategy not only reduced the MIC of MER against *E. coli* (bla_{NDM-1}) and *K. pneumoniae* (bla_{NDM-1}), but also avoided toxicity, making it a safe and effective treatment for resistant Gram-negative bacterial infections.

Declaration of competing interest

The authors declare that they have no known competing financial interests or personal relationships that could have appeared to influence the work reported in this paper.

Ethics statement

All animal procedures were approved by the Ethics Committee for Experimental Research, Shanghai Medical College, Fudan University.

Acknowledgments

This work was funded by the National Natural Science Foundation of China (No. 82073688 to X. Sun and No. 82103971 to Y. Liang), Science and Technology Commission of Shanghai Municipality (No. 21S11907300 to X. Sun), Shanghai Science and Technology Development Fund from Central Leading Local Government (No. YDZX20223100001004 to X. Sun). We thank the National Center for Protein Science in Shanghai for their help with protein mass spectrometry, and Shanghai Junji Medical Laboratory Co., Ltd. for their guidance on bacterial culture. We also thank Prof. Jing Zhang at Huashan Hospital Affiliated to Fudan University for constructive comments on the microdilution MIC assay.

Supplementary materials

Supplementary material associated with this article can be found, in the online version, at doi:10.1016/j.cclet.2022.108072.

References

[1] L. Dortet, L. Poirel, P. Nordmann, BioMed. Res. Int. 2014 (2014) 249856.
[2] N. Guo, Y. Xia, Y. Duan, et al., Chin. Chem. Lett. 34 (2023) 107542.
[3] J. Berkhout, M.J. Melchers, A.C. van Mil, et al., Antimicrob. Agents Chemother. 59 (2015) 2299–2304.
[4] S.J. Hecker, K.R. Reddy, M. Totrov, et al., J. Med. Chem. 58 (2015) 3682–3692.
[5] D.T. King, L.J. Worrall, R. Gruninger, N.C. Strynadka, J. Am. Chem. Soc. 134 (2012) 11362–11365.
[6] J. Brem, R. Cain, S. Cahill, et al., Nat. Commun. 7 (2016) 12406.
[7] G. Bahr, L.J. Gonzalez, A.J. Vila, Chem. Rev. 121 (2021) 7957–8094.
[8] J. Chiou, T.Y. Leung, S. Chen, Antimicrob. Agents Chemother. 58 (2014) 5372–5378.
[9] P.W. Thomas, M. Cammarata, J.S. Brodbelt, W. Fast, ChemBioChem 15 (2014) 2541–2548.
[10] P.W. Thomas, M. Cammarata, J.S. Brodbelt, et al., Biochemistry 58 (2019) 2834–2843.
[11] H. Kurosaki, Y. Yamaguchi, T. Higashi, et al., Angew. Chem. Int. Ed. 44 (2005) 3861–3864.
[12] J. Chiou, S. Wan, K.F. Chan, et al., Chem. Commun. 51 (2015) 9543–9546.
[13] P.W. Thomas, T. Spicer, M. Cammarata, et al., Bioorg. Med. Chem. 21 (2013) 3138–3146.
[14] C. Chen, K.W. Yang, L.Y. Wu, J.Q. Li, L.Y. Sun, Chem. Commun. 56 (2020) 2755–2758.
[15] D. Buttner, J.S. Kramer, F.M. Klingler, et al., ACS Infect. Dis. 4 (2018) 360–372.
[16] P. Linciano, L. Cendron, E. Gianquinto, F. Spyrakis, D. Tondi, ACS Infect. Dis. 5 (2019) 9–34.
[17] H. Xie, J. Mire, Y. Kong, et al., Nat. Chem. 4 (2012) 802–809.
[18] W. Gao, B. Xing, R.Y. Tsien, J. RaoNovel, J. Am. Chem. Soc. 125 (2003) 11146–11147.
[19] S.S. van Berkel, J. Brem, A.M. Rydzik, et al., J. Med. Chem. 56 (2013) 6945–6953.
[20] L. Gambini, C. Baggio, P. Udompholkul, et al., J. Med. Chem. 62 (2019) 5616–5627.
[21] D.N. Heller, D.A. Kaplan, N.G. Rummel, J. von Bredow, J. Agric. Food Chem. 48 (2000) 6030–6035.
[22] M. Kurogochi, S. Nishimura, Y.C. Lee, J. Biol. Chem. 279 (2004) 44704–44712.
[23] X. Li, H. Yang, Y. Teng, et al., Chin. Chem. Lett. 33 (2022) 4223–4228.
[24] C. Chen, Y. Xiang, K.W. Yang, et al., Chem. Commun. 54 (2018) 4802–4805.
[25] M.R. Mehaffey, Y.C. Ahn, D.D. Rivera, et al., Chem. Sci. 11 (2020) 8999–9010.